

Quantum Hall to charge-density-wave phase transitions in ABC-trilayer graphene

Yafis Barlas,¹ R. Côté,² and Maxime Rondeau²

¹*Department of Physics and Astronomy, University of California, Riverside, CA 92521*

²*Département de physique, Université de Sherbrooke, Sherbrooke (Québec), Canada, J1K 2R1*

(Dated: October 10, 2018)

ABC-stacked trilayer graphene's chiral band structure results in three ($n = 0, 1, 2$) Landau level orbitals with zero kinetic energy. This unique feature has important consequences on the interaction driven states of the 12-fold degenerate (including spin and valley) $N = 0$ Landau level. In particular, at many filling factors $\nu_T = \pm 5, \pm 4, \pm 2, \pm 1$ a quantum phase transition from a quantum Hall liquid state to a triangular charge density wave occurs as a function of the single-particle induced LL orbital splitting Δ_{LL} . Experimental signatures of this phase transition are also discussed.

PACS numbers: 73.21.-b, 73.22.Gk, 72.80.Vp

Introduction— When a group of partially filled Landau levels (LLs) with internal flavor indices are nearly degenerate, electron-electron interactions can lead to spontaneous broken symmetries which induce quasiparticle gaps and hence interaction driven integer quantum Hall (IQH) effects [1]. In semiconducting two-dimensional electron systems (2DES) where Zeeman splitting is negligible and the LLs consist of narrowly spaced doublets, interactions lead to spontaneous electron spin polarization [2] accompanied by a large exchange enhanced spin gap. More recently interaction driven broken symmetry states at integer fillings have been observed in both graphene [3, 4] and bilayer graphene [5, 6] which in most cases exhibits a set of four-fold degenerate LLs. At many filling factors this four-fold degeneracy, which is due to the spin and valley degree of freedom, is spontaneously broken resulting in charge gaps and hence incompressible quantum Hall (QH) states. Bilayer graphene's chiral bands lead to an additional degeneracy doubling of the zero-energy LL associated with the $n = 0$ and $n = 1$ LL orbitals [7], leading to an eight-fold degenerate LL. This additional LL degeneracy also results in interaction driven QH effects due to an exchange induced gap between the LL pseudospins [5, 8].

At relevant energy scales few layer graphene with different stacking sequences, referred to as chiral 2DES (C2DES), exhibit electronic properties distinct from semiconducting 2DES [9]. The difference in the LL structure of C2DES is most evident in the zero-energy LL: for certain stacking sequences (such as AB, ABC, ABCB, etc.) multiple LL orbitals are degenerate [10]. The role of interactions on the ground state when multiple LL orbital degrees of freedom are degenerate remains relatively unexplored. In this Letter we show that, unlike bilayer graphene, at certain filling factors interaction induced QH states are unstable in ABC-stacked trilayer graphene's 12-fold degenerate zero-energy LL. This is due to the presence of a degenerate set of triplet ($n = 0, 1, 2$) LL orbitals. While the QH liquid state is stable for $\nu = -3, 3, 6$ the nature of the ground states at $\nu = \pm 5, \pm 4, \pm 2, \pm 1$ depends on the ratio of a single

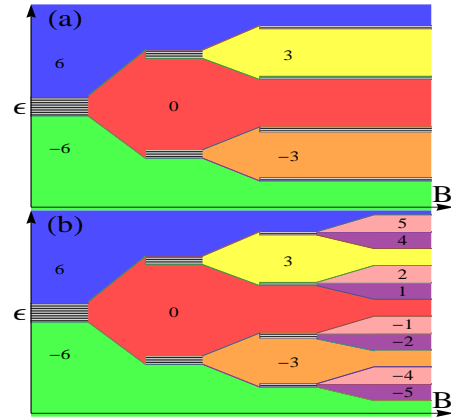


FIG. 1. (Color online) Schematic representation of the interaction induced energy gaps as a function of the magnetic field for interaction driven states in ABC-trilayer graphene's 12-fold degenerate LL, the numbers represent the Hall conductivity in units of e^2/h . For (a) $\Delta_{LL} < \Delta_{LL}^{(c)}$ the presence of insulating triangular CDW states for $\nu = \pm 5, \pm 4, \pm 2, \pm 1$ results in Hall plateaus only at $\sigma_{xy} = \pm 6, \pm 3, 0 (e^2/h)$. For (b) $\Delta_{LL} > \Delta_{LL}^{(c)}$ interaction driven QH states appear at all intermediate integer fillings with the sequence determined by Hund's rule behavior (see text for details).

particle induced LL orbital splitting Δ_{LL} and electron-electron interactions $e^2/\epsilon l_B$ ($l_B = \sqrt{hc/eB}$ is the magnetic length). In particular, a quantum phase transition occurs from a triangular charge density wave (CDW) to a translationally invariant QH liquid state as Δ_{LL} is increased beyond a critical value $\Delta_{LL}^{(c)}$ [12]. This transition is first order in the liquid-solid universality class. The crystal state exhibits coherence between LL orbitals which leads to vortex textures of in-plane electric dipoles at each lattice site. For moderately disordered samples this phase transition should be characterized by a Hall plateau transition as a function of Δ_{LL} at a fixed filling factor ν . Another consequence is that the Hall conductivity for $\Delta_{LL} < \Delta_{LL}^{(c)}$ will correspond to the adjacent interaction driven IQH plateau, for example, at $\nu = -5, -4,$

$\sigma_{xy} = -6e^2/h$ (as shown in Fig. 1a).

ABC-trilayer graphene– ABC-stacked graphene trilayers are chiral generalization of monolayer and Bernal-stacked bilayer graphene. ABC-stacked trilayer is a particular stacking of three graphene layers each with inequivalent sublattices A_i and B_i arranged in following sequence: one of the two-carbon atom sites in both the top and bottom layer $B_1(A_3)$ has a different near-neighbor carbon atom site in the middle layer $A_2(B_2)$, which leaves one-carbon atom site in the top and bottom layers $A_1(B_3)$ without a near-neighbor in the middle layer. Interlayer hopping on adjacent layer near-neighbor carbon atom sites leads to the formation of high-energy dimer bands which push the electron energy away from the Fermi surface leaving one low-energy sublattice site per π -carbon orbital in the outermost layers. Because the hopping between the low-energy sites via intermediate high-energy states is a three-step process, it turns out that in the presence of an external magnetic field three LL orbitals ($n = 0, 1, 2$) have zero kinetic energy. The wavefunctions of the opposite $\mathbf{K}(\mathbf{K}')$ valleys in the zero-energy LL are localized in the top(bottom) layers, hence layer and valley labels are equivalent. This simplified two-band model for the ABC-stacked graphene trilayer which includes only nearest-neighbor interlayer and intralayer hopping terms is valid at large external magnetic fields [15]. The effects of an external potential difference between the top and bottom layers Δ_V along with remote next-nearest interlayer hopping terms on the zero-energy LL, not included in our simplified model, can be incorporated by introducing a symmetric LL gap Δ_{LL} [14] between the degenerate zero-energy triplet set ($n = 0, 1, 2$) of LL orbitals. The effect of these terms on Δ_{LL} will be reported elsewhere [15].

Mean field theory– Trilayer graphene's zero-energy LL is a direct product of two $S = 1/2$ doublets corresponding to spin and valley (layer) pseudospin along with $S = 1$ LL orbital pseudospin which is responsible for the new physics discussed in this Letter. Working in the Landau gauge $\mathbf{A} = (0, Bx, 0)$, the Hartree-Fock (HF) mean-field Hamiltonian, projected onto the zero-energy LL of ABC-stacked trilayer, consists of single particle pseudospin splitting terms along with direct and exchange interaction contributions: $\mathcal{H}_{HF} = \mathcal{H}_{sp} + \mathcal{H}_{int}$, with

$$\begin{aligned} \frac{\mathcal{H}_{int}}{N_\phi} = & \sum_{\mathbf{q} \neq 0, r, s} H_{n_1 n_2 n_3 n_4}^{\alpha\beta}(\mathbf{q}) \langle \Delta_{\alpha s; \alpha s}^{n_1 n_4}(\mathbf{q}) \rangle \Delta_{\beta r; \beta r}^{n_2 n_3}(-\mathbf{q}) \\ & - \sum_{\mathbf{q}, r, s} X_{n_1 n_2 n_4 n_3}^{\alpha\beta}(\mathbf{q}) \langle \Delta_{\alpha s; \beta r}^{n_1 n_4}(\mathbf{q}) \rangle \Delta_{\beta r; \alpha s}^{n_2 n_3}(-\mathbf{q}), \quad (1) \end{aligned}$$

(repeated indices are summed over) where $n_i = 0, 1, 2$ are the LL orbital indices, $\alpha, \beta = t(b)$ label the top (bottom) layers ($\mathbf{K}(\mathbf{K}')$ valleys) and $r, s = 1(-1)$ label the \uparrow (\downarrow) spins, $N_\phi = A/(2\pi l_B^2)$ is the degeneracy of a single LL

and momentum space guiding center density is ,

$$\Delta_{\alpha s; \beta r}^{nn'}(\mathbf{q}) = \frac{1}{N_\phi} \sum_{X, X'} c_{nX\alpha s}^\dagger c_{n'X'\beta r} e^{-i\frac{\mathbf{q}\cdot\mathbf{r}}{2}(X'+X)} \delta_{q_y l_B^2, X-X'}, \quad (2)$$

where $c_{nX\alpha s}^\dagger (c_{nX\alpha s})$ are the respective n^{th} LL creation and annihilation operators at a given guiding center X in the Landau gauge with layer and spin index α, s . The effects of the single-particle pseudospin splitting field are encoded in

$$\frac{\mathcal{H}_{sp}}{N_\phi} = \left(n\Delta_{LL} - \xi_\alpha \frac{\Delta_V}{2} - s \frac{\Delta_Z}{2} \right) \rho_{\alpha s}^n, \quad (3)$$

where $\rho_{\alpha s}^n = \Delta_{\alpha s; \alpha s}^{n, n}(\mathbf{q} = 0) = \sum_X \langle c_{nX\alpha s}^\dagger c_{nX\alpha s} \rangle$ is the total guiding center density for the n^{th} LL with valley and spin index α, s and Δ_{LL} is the LL splitting induced by the remote interlayer hopping terms and the external potential difference Δ_V with $\xi_{t(b)} = 1(-1)$, $\Delta_Z = g\mu_B B$ is the Zeeman splitting and all energies are measured in units of $e^2/\epsilon l_B$. In (1) the Hartree-field captures the valley (layer) dependent electrostatic contributions:

$$H_{n_1 n_2 n_3 n_4}^{\alpha\beta}(\mathbf{q}, d) = \frac{1}{2\pi l_B^2} v_{\mathbf{q}}^{\alpha\beta} F_{n_1 n_4}(\mathbf{q}) F_{n_2 n_3}(-\mathbf{q}), \quad (4)$$

and the exchange contribution is captured by:

$$\begin{aligned} X_{n_1 n_2 n_3 n_4}^{\alpha\beta}(\mathbf{q}, d) = & \frac{1}{L^2} \sum_{\mathbf{p}} v_{\mathbf{p}}^{\alpha\beta} F_{n_1 n_4}(\mathbf{p}) F_{n_2 n_3}(-\mathbf{p}) \\ & \times e^{i(\mathbf{p} \times \mathbf{q}) l_B^2}, \quad (5) \end{aligned}$$

where $v_{\mathbf{q}}^{tt} = v_{\mathbf{q}}^{bb} = 2\pi e^2/\epsilon|\mathbf{q}|$ and $v_{\mathbf{q}}^{tb} = v_{\mathbf{q}}^{bt} e^{-qd}$ [16] is the Fourier transform of electron-electron interactions in the same and different layers (valleys) and $d = 0.667\text{nm}$ is the interlayer separation. The form factors $F_{nn'}(\mathbf{q})$ capture the character of the three different LL orbitals and are given by:

$$F_{nn'}(\mathbf{q}) = \sqrt{\frac{n!}{n'}} \left(\frac{i|q|e^{i\theta_q l_B}}{\sqrt{2}} \right)^{n-n'} L_{n'-n}^{n-n'} \left(\frac{(ql_B)^2}{2} \right) e^{-\frac{(ql_B)^2}{4}}, \quad (6)$$

for $n' \leq n$, where $L_n^\alpha(x)$ is the generalized Laguerre polynomial, $\theta_q = \tan^{-1}(q_y/q_x)$ and the form factors satisfy $F_{nn'}(\mathbf{q}) = [F_{n'n}(-\mathbf{q})]^*$.

First we look for translationally invariant solutions of the density matrix $\langle \Delta_{\alpha s; \alpha' s'}^{n, n'}(\mathbf{q} = 0) \rangle$. The density matrix must be determined by self-consistently occupying the lowest energy eigenvectors of \mathcal{H}_{HF} . For a uniform density order parameter the only contribution to the Hartree term is $E_H = (e^2/\epsilon l_B)(d/2l_B)$, which captures the charging capacitance energy of the outermost layers of ABC-trilayers. The filling order of the 12-fold degenerate zero-energy LL proceeds in integer increments starting from the filling factor $\nu = -6$ and follows a Hund's rule behavior: first maximize spin polarization, then maximize the layer pseudospin polarization to the greatest possible

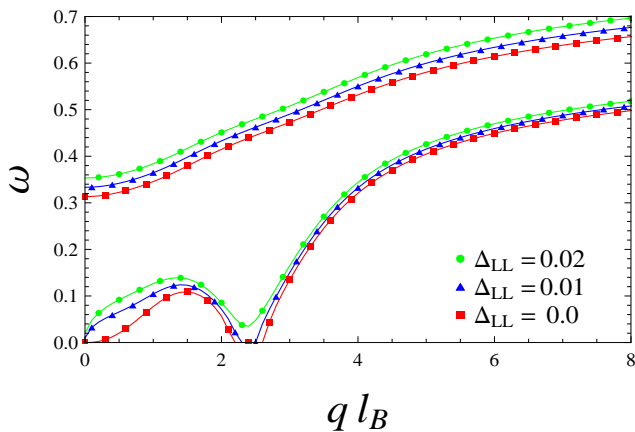


FIG. 2. (Color online) Collective mode dispersion ω_q for $\nu = -5, -2, 1, 4$ in units of interaction strength $e^2/\epsilon l_B = 11.2(B[T])^{1/2}$ meV as a function of ql_B at different values of the LL splitting Δ_{LL} at a magnetic field of $B = 10$ Tesla. Charge density wave instability is accompanied by a softening of the magneto-roton minima for $\Delta_{LL} \leq \Delta_{LL}^*$. The gapped mode corresponds to the hard-direction in LL pseudospin space and is not essential for our discussion (see text for details).

extent and finally maximize the LL polarization to the greatest extent allowed by the first two rules (see Fig. 1b).

For balanced ABC-trilayers ($\Delta_V = 0$) at $\nu = -3, 3$ the valley(layer) pseudospin exhibits spontaneous inter-valley(layer) coherent state similar to that observed in conventional 2DEGs [18]. The $\nu = 0$ state is spin polarized as the exchange gap associated with spin polarization is larger than the exchange gap associated with the inter-layer coherent state. However, since the energy scales associated with Zeeman splitting and the ratio d/l_B are small compared to typical interaction energies, the valley and spin exchange gaps compete closely which could alter the Hund's rule behavior (for example leading to density wave states rather than spin-polarized states at $\nu = 0$). Another consequence of a small value of d/l_B is that for a small value of $\Delta_V (\geq (\pi/8)^{1/2}(d/l_B)^2 e^2/\epsilon l_B)$ the inter-layer coherent state switches to a valley polarized state.

Hund's rule dictate that the topmost LLs at $\nu = -5, -2, 1, 4$ have $n = 0$ LL orbital occupation whereas at $\nu = -4, -1, 2, 5$ the $n = 1$ LL orbital is occupied. This preference of LL orbital occupation is associated with a better exchange energy of the more localized $n = 0$ LL orbital wavefunction along with the absence of nodes [5]. The new physics discussed in this Letter is primarily associated with the LL pseudospin ordering at $\nu \neq -3, 0, 3, 6$. In the next section we show that for $\Delta_{LL} < \Delta_{LL}^*$ the translationally invariant uniform liquid QH states at $\nu = -5, -2, 1, 4$ are unstable to the LL orbital fluctuations. This instability is due to strong

charge fluctuations which lead to a softening of the collective mode dispersion as a function of Δ_{LL} .

Charge density wave instability—We now focus on the collective excitations of a filled QH liquid at filling factors $\nu = -5, -2, 1, 4$, freezing spin, and valley (layer) but keeping the ($n = 0, 1, 2$) LL orbital degrees of freedom. To further simplify the discussion and concentrate on the LL pseudospin fluctuations, we also assume SU(4)-invariant spin and valley (layer) independent interactions. [19] In this case the SU(4)-flavor index is spontaneously broken and quantized LL pseudospin fluctuation consists of pseudospin rotations which mix $n = 0$ with $n = 1$ and $n = 2$ LL orbitals leading to two branches of collective mode excitations. The collective mode excitations which we evaluate below are primarily influenced by the orbital dependence of the microscopic Hamiltonian (1). A detailed account of the collective excitations for $d \neq 0$ will be presented elsewhere [15].

One physically transparent way of performing these collective mode calculations is to construct a fluctuation action in which each transition has canonically conjugate density ρ and phase φ components corresponding to the real and imaginary parts of the final state component in the fluctuating spinor. The fluctuation action

$$\mathcal{S}[\rho, \varphi] = \mathcal{S}_B[\rho, \varphi] - \int d\omega \int d^2q \mathcal{E}[\rho, \varphi], \quad (7)$$

contains a Berry phase term \mathcal{S}_B [20]

$$\mathcal{S}_B[\rho, \varphi] = \int d\omega \int d^2q \left[\frac{1}{2} \rho_{-\mathbf{q}}^\dagger \mathcal{D} \varphi_{\mathbf{q}} - \varphi_{-\mathbf{q}}^\dagger \mathcal{D}^\dagger \rho_{\mathbf{q}} \right], \quad (8)$$

where $\mathcal{D} = -i\omega \mathbb{1}_{2 \times 2}$ and $\rho_{\mathbf{q}} = (\rho_{1,\mathbf{q}}, \rho_{2,\mathbf{q}})$ with $\rho_{n,\mathbf{q}}$ corresponding to the charge fluctuation of the $n = 0$ to the n^{th} orbital, with a similar definition for the phase variable $\varphi_{\mathbf{q}}$. The energy functional, $\mathcal{E}[\rho, \varphi]$ is closely related to the discussion in the preceding section

$$\mathcal{E}[\rho, \varphi] = \frac{1}{2} \left[\rho_{-\mathbf{q}}^\dagger (\Gamma_q + \Lambda_q) \rho_{\mathbf{q}} + \varphi_{-\mathbf{q}}^\dagger (\Gamma_q - \Lambda_q) \varphi_{\mathbf{q}} \right]. \quad (9)$$

Here, Γ_q and Λ_q are 2×2 Hermitian matrices which capture the energy cost of small pseudospinor fluctuations and can be evaluated explicitly. The matrix elements of Γ_q can Λ_q can be expressed in terms of direct and exchange matrix elements:

$$\begin{aligned} \gamma_{ij} &= a_i \delta_{ij} + (-1)^{i+j} H_{i0j0}(|\mathbf{q}|, 0) - X_{i0j}(\mathbf{q}, 0), \\ \lambda_{ij} &= (-1)^{i+j} H_{i0j0}(|\mathbf{q}|, 0) - X_{00ij}(\mathbf{q}, 0), \end{aligned} \quad (10)$$

where $a_1 = \Delta_{LL} + 1/2\sqrt{\pi/2}$ and $a_2 = 2\Delta_{LL} + 5/8\sqrt{\pi/2}$ are wavevectors independent contributions measured in units of $e^2/\epsilon l_B$.

The collective mode dispersion plotted in Fig. 2 indicates that the uniform QH liquid state is unstable for $\Delta_{LL} \leq \Delta_{LL}^* = 0.015e^2/(\epsilon l_B)$. The gapped mode in Fig. 2 which corresponds to some wavevector dependent

linear combination of the orbital pseudospin fluctuations ($\rho_{n,\mathbf{q}}, \varphi_{n,\mathbf{q}}$) reflects the difference in the exchange energy cost of the LL orbitals. The “soft-mode” indicates the instability of the uniform QH liquid at $q_0 l_B \sim 2.37$ which is due to the charge fluctuations of the QH liquid as we show next.

In order to analyze this instability and its associated consequences it is convenient to expand the energy functional of the “soft-mode” density $\rho_{-, \mathbf{q}}$ near $q \sim q_0$,

$$\mathcal{E}[\rho_{-, \mathbf{q}}] = [\alpha(\Delta_{LL}) + \xi(\Delta_{LL})(q - q_0)^2] \rho_{-, \mathbf{q}}^2 \quad (11) \\ + \beta(\Delta_{LL}) \rho_{-, \mathbf{q}_1} \rho_{-, \mathbf{q}_2} \rho_{-, \mathbf{q}_3} \delta(\mathbf{q}_1 + \mathbf{q}_2, \mathbf{q}_3) + \dots$$

where $\alpha(\Delta_{LL}) = 1.24(\Delta_{LL} - \Delta_{LL}^{(*)})$ with $\xi(\Delta_{LL}) = 0.29 - 0.14\Delta_{LL}$ and $\beta(\Delta_{LL})$ is the coefficient of the third order term which is not prohibited by any symmetries. For $\beta = 0$ (11) exhibits a Brazovskii-like instability leading to a fluctuation-induced isotropic-smectic transition to a unidirectional LL-pseudospin density wave pattern [21]. However, the presence of a finite β preempts this transition to a triangular two-dimensional CDW (or crystal)[22] with LL orbital pseudospin textures.

This instability should be present whenever ($n \geq 2$) LL orbitals are degenerate. The effective interaction within the projected n^{th} LL orbital $v_n(q) = v_q [L_n(q^2 l_B^2 / 2)]^2 e^{-q^2 l_B^2 / 2}$ has minimas corresponding to zeros of the Laguerre polynomials. Due to this the Hartree contribution vanishes at these finite- q wavevectors and since the exchange energy is positive for all wavevectors, E_{HF} becomes negative [23]. The near degeneracy of $n = 0, 1, 2$ LL orbitals allows electrons access to lower energy by forming coherent superposition of LL orbitals for a range of finite- q wavevectors, leading to a CDW instability. As Δ_{LL} is increased from below this gain in energy competes with the single particle contribution and the uniform QH state becomes energetically more favorable resulting in a transition.

Triangular Charge Density Wave ($\Delta_{LL} < \Delta_{LL}^c$)— For $\Delta_{LL} < \Delta_{LL}^{(c)}$ with $\Delta_{LL}^{(c)} = 0.095e^2/\varepsilon l_B > \Delta_{LL}^{(*)}$ at $\nu = -5, -2, 1, 4$, the HF solution with the lowest energy is a triangular crystal of electrons with one electron per lattice site as shown in Fig. 3 [24]. In this crystal state, all three orbitals $n = 0, 1, 2$ are occupied in contrast with the QH liquid state where only $n = 0$ is fully occupied. As $\Delta_{LL} \rightarrow \Delta_{LL}^{(c)}$ from below, the total population $\langle \Delta_{1,1} \rangle + \langle \Delta_{2,2} \rangle$ of the higher-energy orbitals decreases but stays finite until $\Delta_{LL}^{(c)}$ where it drops discontinuously to zero indicating a first order transition to the liquid state with $\langle \Delta_{0,0} \rangle = 1$. At each crystal site, the electron is in a superposition of the three orbital states $n = 0, 1, 2$. Since the wavefunction profile of the three orbitals is different, this superposition leads to the triangular CDW pattern in the total electron density $n(\mathbf{r})$ shown in Fig. 3 (a). When two orbital are filled (at $\nu = -4, -1, 2, 5$ for example), the ground state at small Δ_{LL} is a crystal of holes instead of electrons (see Fig3 (b)).

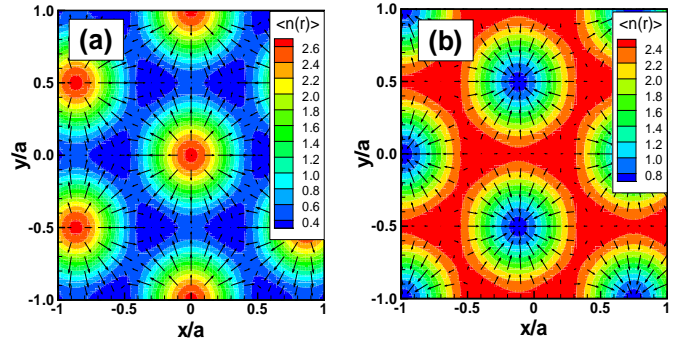


FIG. 3. (Color online) Electronic density and orientation of the in-plane electric dipole field for the triangular crystal at filling factor (a) $\nu = -5, -2, 1, 4$ and (b) $\nu = -4, -1, 2, 5$. The electrons for (a) and holes for (b) crystallize in a triangular pattern with a lattice constant $a = \sqrt{4\pi/\sqrt{3}}l_B$. The crystal state is characterized by a superposition of three LL orbitals $n = 0, 1, 2$ pseudospin which manifests itself as a periodic density modulation $n(\mathbf{r})$ (see text for details).

The CDW state is characterized by a periodic modulation of $\langle \Delta_{n,m}(\mathbf{q}) \rangle$ ($n \neq m$) defined in Eq. (2). This leads to the presence of an in-plane electric dipole field (a similar situation also occurs in bilayer graphene[25]):

$$d_{i=x,y}(\mathbf{q}) = -\sqrt{2}el_B e^{-q^2 l_B^2 / 4} \langle \rho_i^{(0,1)}(\mathbf{q}) \rangle \quad (12) \\ - 2el_B e^{-q^2 l_B^2 / 4} (1 - q^2 l_B^2 / 4) \langle \rho_i^{(1,2)}(\mathbf{q}) \rangle,$$

where $\rho_x^{(n,m)} = (\Delta_{n,m} + \Delta_{m,n})/2$, $\rho_y^{(n,m)} = (\Delta_{n,m} - \Delta_{m,n})/2i$ (with $n > m$), the energy of the CDW state in the presence of an external electric field is $-\int d\mathbf{r}(\mathbf{d}(\mathbf{r}) \cdot \mathbf{E}(\mathbf{r}))$. Fig. 3(a)-(b) also show the orientation of the in-plane electric dipole field around each crystal site which exhibits vortex textures in which the dipole vectors rotate by 2π . The topological properties of this crystal state will be characterized elsewhere [15].

The degeneracy of $n = 2$ LL orbital is crucial for the existence of the crystal state. This situation is somewhat reminiscent of the various crystal phases that appear in conventional 2DES at fractional fillings of higher LLs $n \geq 2$ [23, 26]. The surprising result here is that similar electronic crystal phases appear at total *integer* filling factors in ABC-stacked trilayer graphene and are sensitive to the competition of interactions and single particle terms induced by remote hopping and layer imbalance. This triangular CDW state would likely be pinned by disorder leading to insulating behavior of the uppermost LL thus exhibiting quantized Hall conductivity at a value corresponding to the *adjacent* interaction driven IQH plateau (see Fig. 1a). The triangular CDW state should also be visible through its pinning mode in microwave absorption experiments.

Acknowledgements: The authors would like to thank C. M. Varma and A. H. MacDonald for many fruitful discussions and comments on the manuscript. R. Côté was supported by Natural Sciences and Engineering Research Council of Canada (NSERC), Compute Canada and Calcul Québec.

-
- [1] S. M. Girvin and A. H. MacDonald, Chap. 5 in *Perspectives in Quantum Hall Effects*, Edited by Sankar Das Sarma and Aron Pinczuk (Wiley, New York, 1997).
- [2] S. L. Sondhi, A. Karlhede, S. A. Kivelson and E.H. Rezayi, Phys. Rev. B **47**, 16419 (1993).
- [3] Y. Zheng *et. al.* Phys. Rev. Lett. **96**, 136806 (2006).
- [4] K. Nomura and A. H. MacDonald, Phys. Rev. Lett. **96**, 256602 (2006).
- [5] Y. Barlas, R. Côté, K. Nomura and A. H. MacDonald, Phys. Rev. Lett. **101**, 097601 (2008).
- [6] R. T. Weitz *et. al.* Science **330**, 812 (2010); Y Zhao *et. al.* Phys. Rev. Lett. **104**, 066801 (2010).
- [7] E. McCann and V. I. Falko, Phys. Rev. Lett. **96**, 086805 (2006).
- [8] Y. Barlas, R. Côté, J. Lambert and A. H. MacDonald, Phys. Rev. Lett. **104**, 096802 (2010)
- [9] Hongki Min and A. H. MacDonald, Phys. Rev. B **77**, 155416 (2008).
- [10] Y. Barlas, K. Yang, A. H. MacDonald, Nanotechnology, **23** 052001 (2012).
- [11] L. Zhang, Nat. Phys. **7**, 953 (2011); W. Bao, *et. al.*, Nat. Phys. **7**, 948 (2011); A. Kumar, *et. al.*, Phys. Rev. Lett. **107**, 126806 (2011).
- [12] Δ_{LL} can be increased by applying an external potential difference Δ_V between the outermost layers.
- [13] Fan Zhang, Bhagawan Sahu, Hongki Min, and A. H. MacDonald, Phys. Rev. B **82**, 035409 (2010).
- [14] In this Letter we require a symmetric $0 \leq \Delta_{LL} < 0.3e^2/\epsilon l_B$. The phase diagram for $\Delta_{LL} < 0$ and for an asymmetric LL orbital splitting will be reported elsewhere [15].
- [15] R. Côté, Maxime Rondeau and Y. Barlas, in preparation.
- [16] Due to the fact that LL-spacing $\omega_c \sim B^{3/2}$ and interactions $V_{e-e} \sim \sqrt{B}$ it is sufficient to consider unscreened Coulomb interactions (see supplemental material).
- [17] H. A. Fertig, Phys. Rev. B **40**, 1087 (1989); A. H. MacDonald, P. M. Platzman and G. Boebinger, Phys. Rev. Lett. **65**, 775 (1990); K. Moon *et. al.* Phys. Rev. B **51**, 5138 (1995).
- [18] I. B. Spielman, J. P. Eisenstein, L. N. Pfeiffer, and K. W. West Phys. Rev. Lett. **84**, 5808 (2000)
- [19] This approximation is well justified since the layer separation is merely a fraction of a nanometer.
- [20] See, for example, Assa Auerbach, *Interacting Electrons and Quantum Magnetism* (Springer, New York, 1994).
- [21] S. A. Brazovskii, Zh. Eksp. Teor. Fiz. 68, 175 (1975) [Sov. Phys. JETP 41, 85 (1975)]; P. C. Hohenberg and J. B. Swift, Phys. Rev. E 52, 1828 (1995).
- [22] S. Alexander and J. McTague, Phys. Rev. Lett. **41**, 701 (1978).
- [23] A. A. Koulakov, M. M. Fogler and B. I. Shklovskii, Phys. Rev. Lett. **79**, 499 (1996).
- [24] Laughlin-like correlated states cannot be captured in our HF approximation and require an exact diagonalization approach which remains technically challenging for the case of multiple LL orbitals.
- [25] K. Shizuya, Phys. Rev. B **79**, 165402 (2009); R. Côté, Wenchen Luo, Branko Petrov, Yafis Barlas and A. H. MacDonald, Phys. Rev. B **82**, 245307 (2010); R. Côté, J. P. Fouquet, and Wenchen Luo, Phys. Rev. B **84**, 235301 (2011).
- [26] M. P. Lilly *et. al.* Phys. Rev. Lett. **82**, 394 (1999).